## 4.0 RESULTS AND DISCUSSIONS

Scanning electron microscopy (SEM) of binder and precipitated silica catalysts are shown in Figure 3. The catalyst is roughly spherical in shape, typical of a spray drying process, with diameters ranging from 30 to 90 μm.

The attrition resistance of the silica binder based catalysts (with no precipitated silica) increased (attrition reduced) as binder level was increased up to 12 % as shown in Table 2. It then decreased when the binder level was increased to 20 %, indicating an optimum binder level of about 10 to 12 %. For this reason, this material was used as the basis for preparing the Fe-pSi(y) series of catalysts with various levels of precipitated silica. The Fe-pSi series containing precipitated silica was prepared with 12 % binder silica. As precipitated silica content increased from 5 to 20 parts by weight, the attrition became so severe that it plugged the attrition tester during 5 h test. It is clear that from these results, the addition of precipitated silica causes more attrition. An HPR series of proprietary catalysts was prepared to further improve attrition resistance. As can be seen, these catalysts have significantly improved attrition resistance, even better than the Fe-bSi series of catalysts. Finally, an HPR-43 material was prepared as a larger 500-g batch to demonstrate scalability of the proprietary preparation technique.

Table 3 shows the BET surface areas of the fresh and reduced catalysts, the hydrogen uptake, pore volume, bulk density and the porosity of all the catalysts synthesized. The BET surface area of the catalysts increased with both binder silica and precipitated silica concentration. In general, the addition of silica to iron FT catalysts is known to improve stability of the porous iron oxide/hydroxide network (Bukur et al., 1995a). Silica enters the pores of the original network of the catalysts, thus providing a rigid matrix which helps prevent a complete collapse of the pore structure of the catalyst. However, after reduction with CO at 280°C for

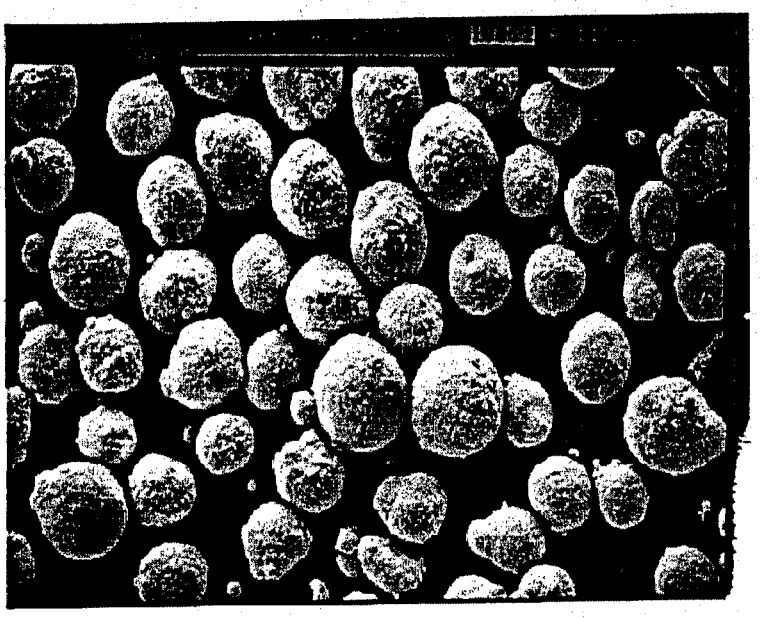

Fig.3 (a)

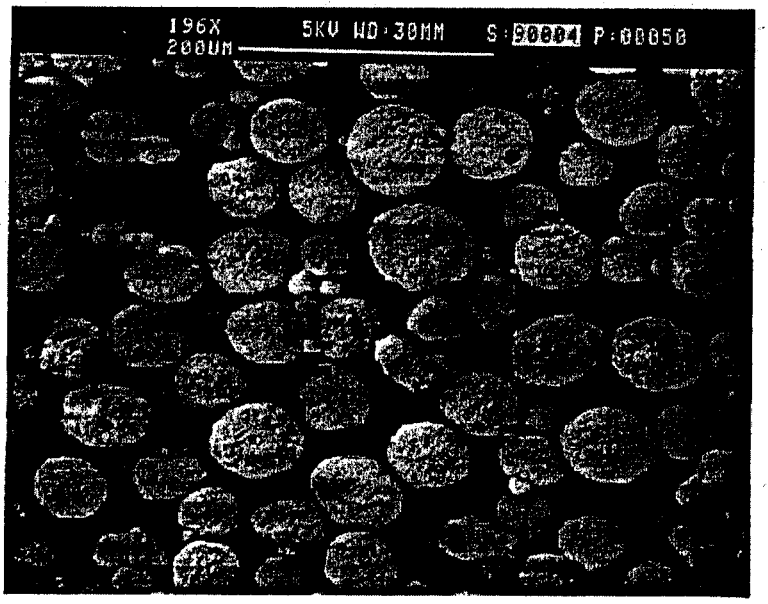


Fig. 3 (b)

Figure 3. SEM Image of the Spray Dried Precipitated Iron Catalysts (a) Fe-bSi(12) (b) Fe-pSi(15)

Table 2. ASTM Fluid Bed Test Results

| Catalyst Designation | Attrition loss (wt %) | |
|---|---|---|
| | 1 h | 5 h |
| Fe-bSi(4) | 24.4 | 32.6 |
| Fe-bSi(8) | 25.7 | 35.4 |
| Fe-bSi(12) | 12.8 | 22.7 |
| Fe-bSi(16) | 22.0 | 30.1 |
| Fe-bSi(20) | 34.9 | 35.0 |
| Fe-pSi(5) | 24.2 | 37.3 |
| Fe-pSi(10) | 31.0 | 39.6 |
| Fe-pSi(15) | 42.1 | * |
| Fe-pSi(20) | 39.1 | * |
| HPR-39 | 4.7 | 10.0 |
| HPR-40 | 4.1 | 9.7 |
| HPR-41 | 6.4 | 17.7 |
| HPR-42 | 5.2 | 15.5 |
| HPR-43 | 7.6 | 14.6 |
| Ruhrchemie | NM | NM |

NM=Not measured

* Tester plugged due to severe attrition

Table 3. Physical and Chemical Properties of Fe Catalysts

| Catalyst Designation | BET Surface Area, $m^2/g$ | | TPR Measurements $H_2$ Desorbed, mmol/g.cat | Pore Volume, mL/g | Bulk Density, g/mL | Porosity, % |
|---|---|---|---|---|---|---|
| | Fresh | Reduced | | | | |
| Fe-bSi(4) | 80.3 | 35.6 | 24.3 | NM | NM | NM |
| Fe-bSi(8) | 95.7 | 50.8 | 23 | NM | NM | NM |
| Fe-bSi(12) | 121 | 68.7 | 20.6 | NM | NM | NM |
| Fe-bSi(16) | 151 | 103 | 19 | NM | NM | NM |
| Fe-bSi(20) | 172 | 98.9 | 18.4 | NM | NM | NM |
| Fe-pSi(5) | 163 | 116 | 18.8 | 0.54 | 0.95 | 51.3 |
| Fe-pSi(10) | 168 | 144 | 17.9 | 0.54 | 0.89 | 48.5 |
| Fe-pSi(15) | 189 | 163 | 17.7 | 0.62 | 0.95 | 59.8 |
| Fe-pSi(20) | 218 | 181 | 17.6 | 0.64 | 0.92 | 58.2 |
| HPR-39 | 107.8 | NM | NM | NM | NM | NM |
| HPR-40 | 81.4 | NM | NM | NM | NM | NM |
| HPR-41 | 60.5 | NM | NM | NM | NM | NM |
| HPR-42 | 79.8 | NM | NM | NM | NM | NM |
| HPR-43 | 81.5 | NM | NM | 0.11 | 2.41 | 27.4 |
| Ruhrchemie | 300 | NM | NM | NM | NM | NM |

NM=Not measured

16 h, the surface area of the reduced catalyst was lower than that of the fresh catalyst. This may be due to the formation of carbonaceous deposits, which causes blocking of the pores of the catalyst. The catalysts prepared had pore volumes in the 0.54 to 0.65 $cm^3/g$ range and the bulk densities in the 0.89 to 0.95 $g/cm^3$ range. These densities are higher than typical precipitated catalysts that have bulk densities of about 0.7 $g/cm^3$ and should allow easier separation from wax which has a density of about 0.68 $g/cm^3$.

The reduction behavior of the FT catalysts was studied by TPR and the profiles for binder and precipitated silica catalysts are shown in Figure 4. There were slight variations among the catalysts, with all showing peaks at 320 and 750°C. The peak at 320°C corresponds to the reduction of $Fe_2O_3 \rightarrow Fe_3O_4$, and the peak at 750°C corresponds to the reduction of $Fe_3O_4$ to metallic iron. Thus, it can be seen that the reduction of $Fe_3O_4$ to Fe is more difficult step requiring temperatures greater than 600°C for its occurrence in temperature-programmed mode. The small shoulder peak at roughly 250°C is due to the reduction of $CuO \rightarrow Cu$. A summary of the TPR characterization results for all the catalysts studied is given Table 3. The hydrogen uptake generally decreased with silica content, though the effect of the precipitated silica is much less than the effect of the binder silica. The higher $H_2$ consumption by the Fe-bSi catalysts compared to the Fe-pSi indicates a greater extent of reduction for catalysts containing binder silica.

X-ray powder diffraction patterns of the fresh, CO-activated sample after activation, and after 100 h of FT synthesis for the binder and precipitated silica catalysts are shown Figures 5 and 6. The pattern has been plotted over $2\theta$ value ranging from 5° to 75°. The pattern in Figures 5 and 6 shows that the "fresh" samples are identical and are comprised of $\alpha$-$Fe_2O_3$. The catalyst activated at 280°C, with CO for 16 h exhibits the peaks for $Fe_3O_4$ and $\chi Fe_{2.5}C$. The "used"

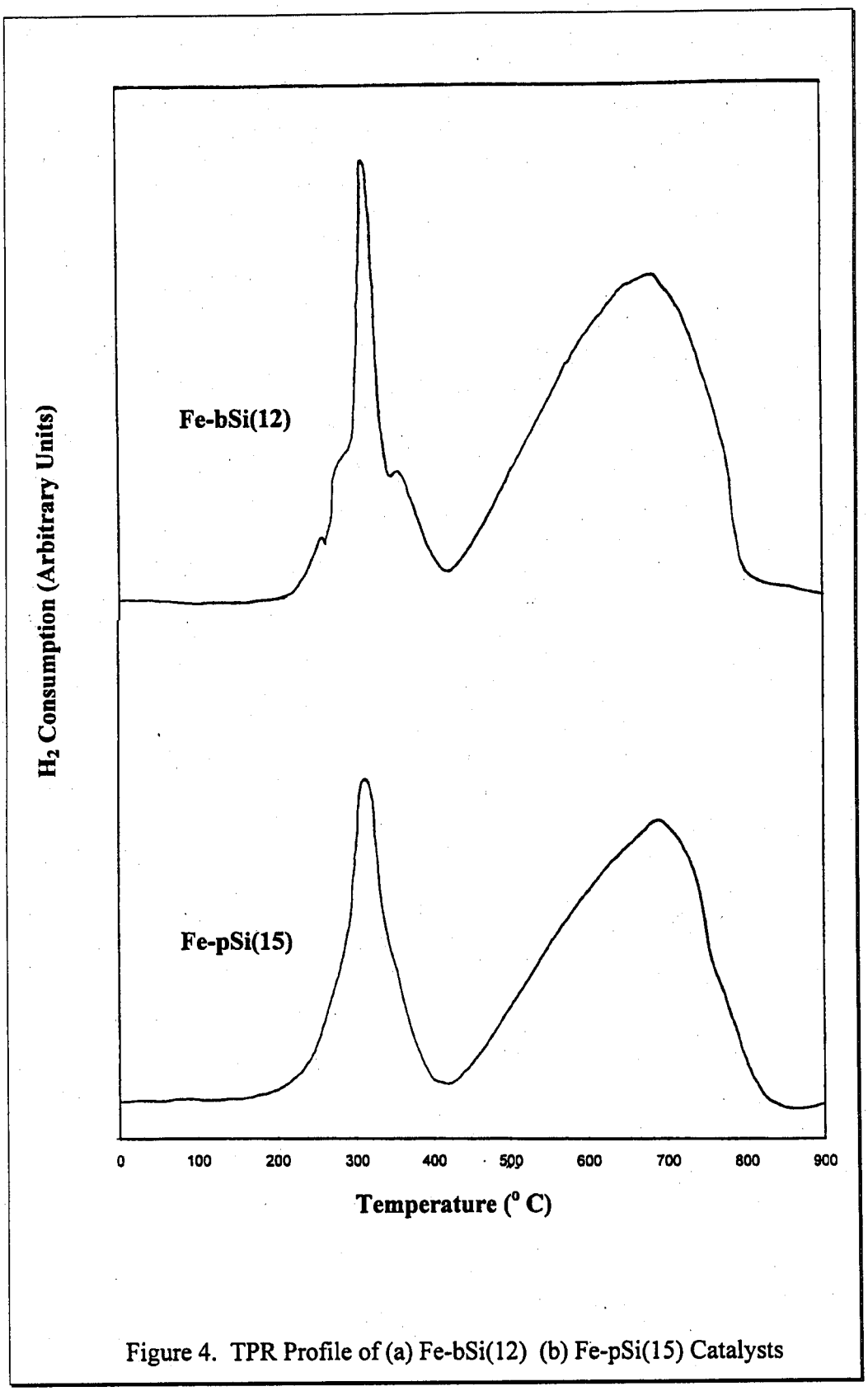


Figure 4. TPR Profile of (a) Fe-bSi(12) (b) Fe-pSi(15) Catalysts

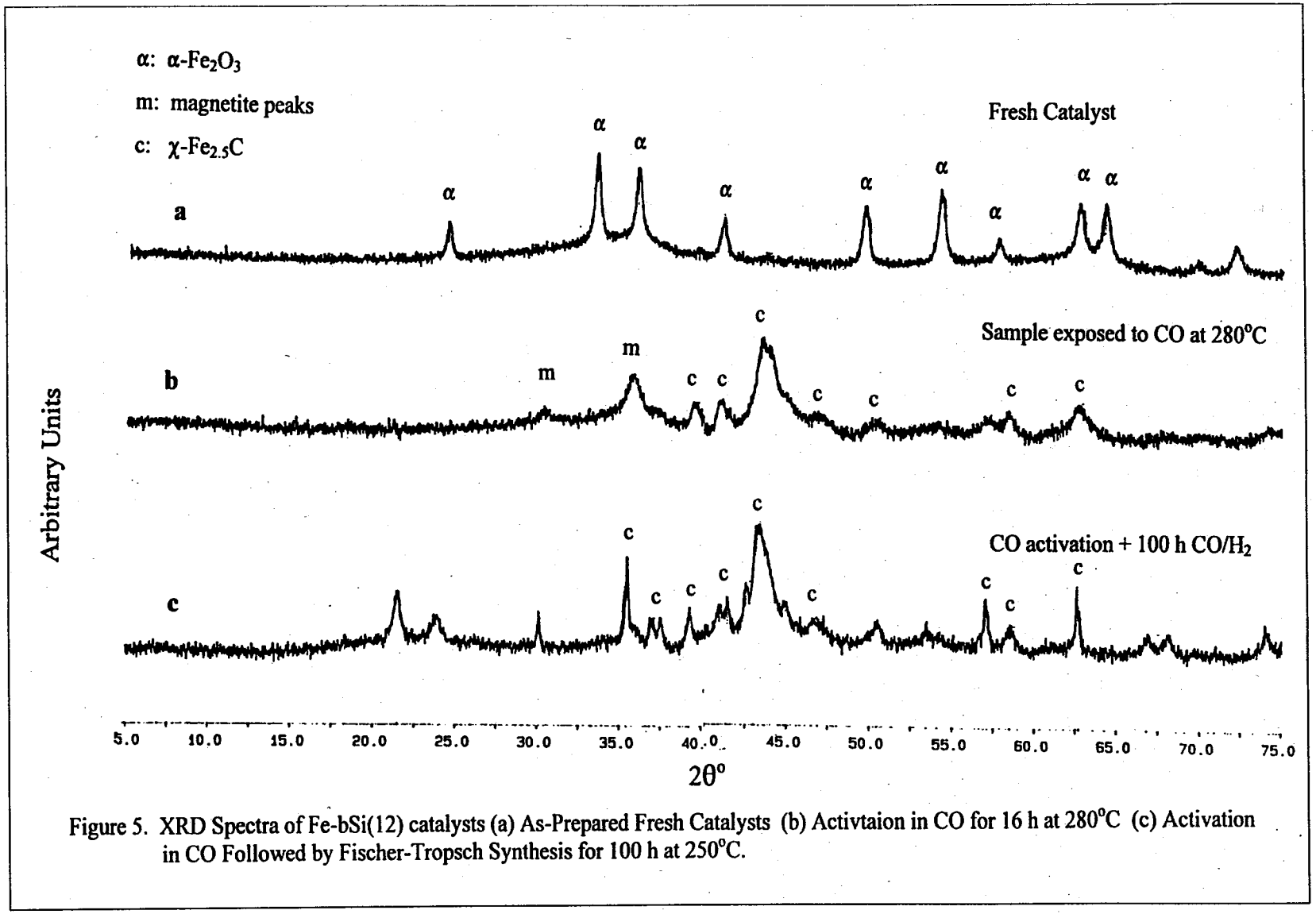


Figure 5. XRD Spectra of Fe-bSi(12) catalysts (a) As-Prepared Fresh Catalysts (b) Activtaion in CO for 16 h at 280°C (c) Activation in CO Followed by Fischer-Tropsch Synthesis for 100 h at 250°C.

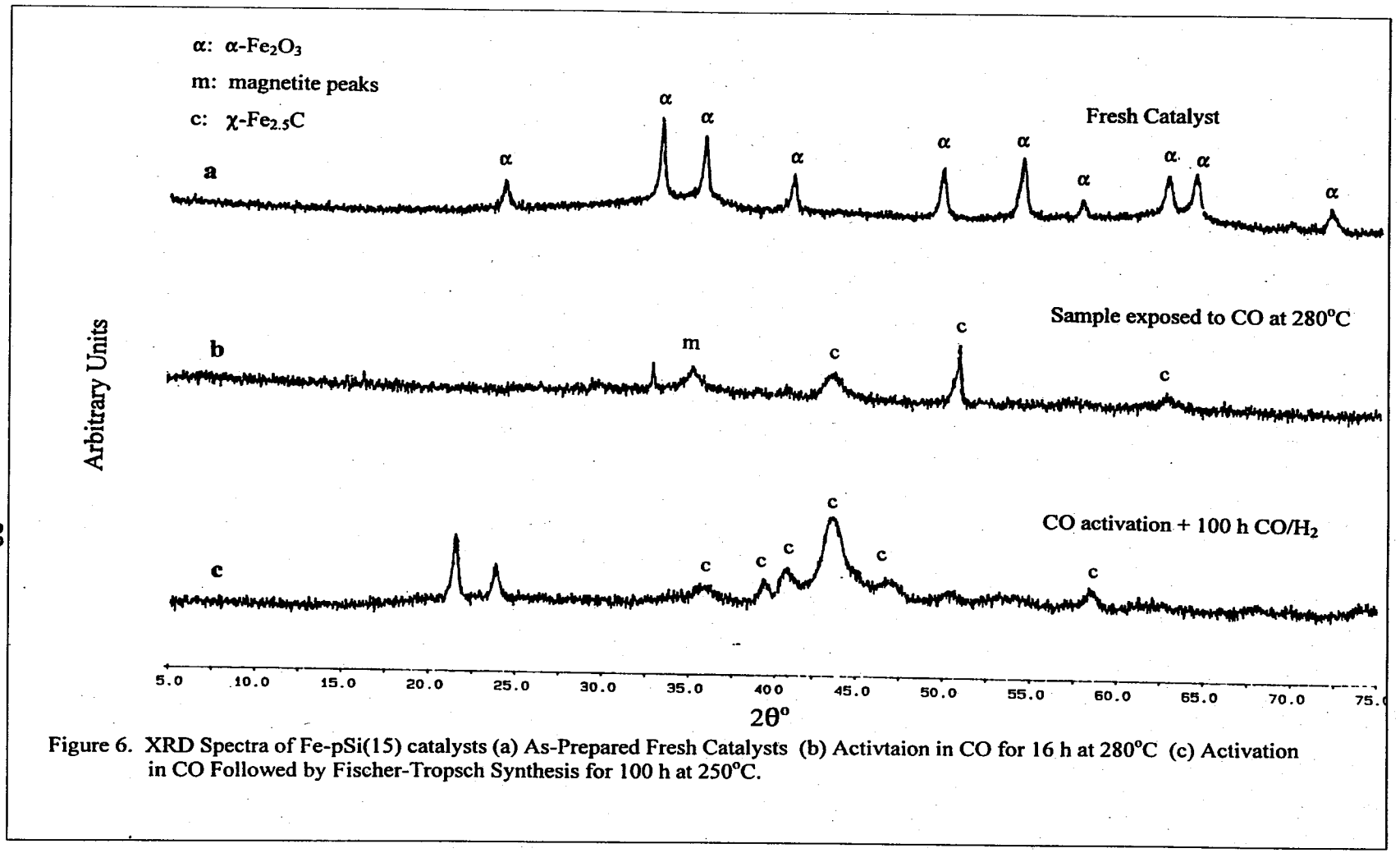


Figure 6. XRD Spectra of Fe-pSi(15) catalysts (a) As-Prepared Fresh Catalysts (b) Activtaion in CO for 16 h at 280°C (c) Activation in CO Followed by Fischer-Tropsch Synthesis for 100 h at 250°C.

sample contain mainly $Fe_{2.5}C$.

The CO conversions plot are shown Figures 7 and 8. All catalysts tested were more active than the Ruhrchemie catalyst. Table 4 shows the CO conversion and hydrocarbon selectivity for the various catalysts, along with the data on Ruhrchemie catalyst for comparison. Following a short induction period, during which steady state was achieved, there was no significant change with time in CO conversions or hydrocarbon selectivities reported in Table 4 over the test duration, typically 100 to 125 h, for any of the catalysts. The alpha value for all catalysts tested range from 0.87 to 0.91. All catalysts tested were more active than Ruhrchemie. The selectivity varied with silica type and content. There was a beneficial effect of binder silica up to 8 to 12 % on selectivity (reduced methane, nearly constant $C_5^+$). However, as binder silica content increased above 12 %, the $C_1$ and $C_2$ to $C_4$ selectivities increased at the expense of $C_5^+$ selectivity. As the precipitated silica content increased (at 12 wt % binder silica), the selectivity to $C_1$ to $C_{11}$ products increased. However, the $C_5$ to $C_{11}$ selectivity for the catalysts containing precipitated silica was higher than the selectivity for those catalysts containing only binder silica.

HPR-43, a proprietary catalyst, showed the lowest methane selectivity and nearly the highest CO conversion. As stated earlier, this catalyst was scaled up to 500-g quantity. This catalyst showed 95 % CO conversion over 125 h of testing at 250°C, 1.48 MPa, and 2 NL/g.cat/h and had a less than 4 % methane selectivity. Its attrition resistance was one of the highest among the catalysts tested.

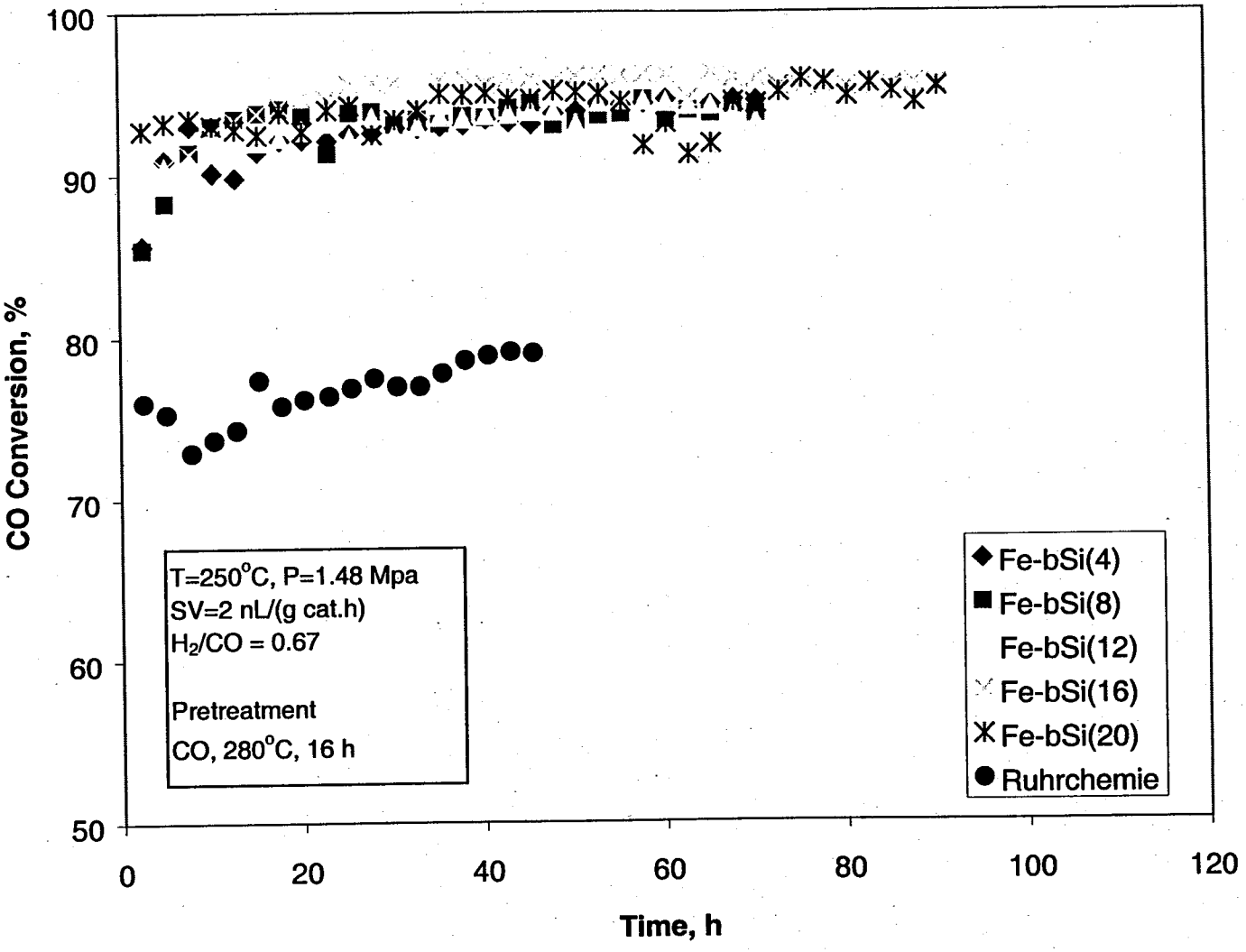


Figure 7. Effect of Binder Silica on Synthesis Gas Conversion and Catalyst Stability

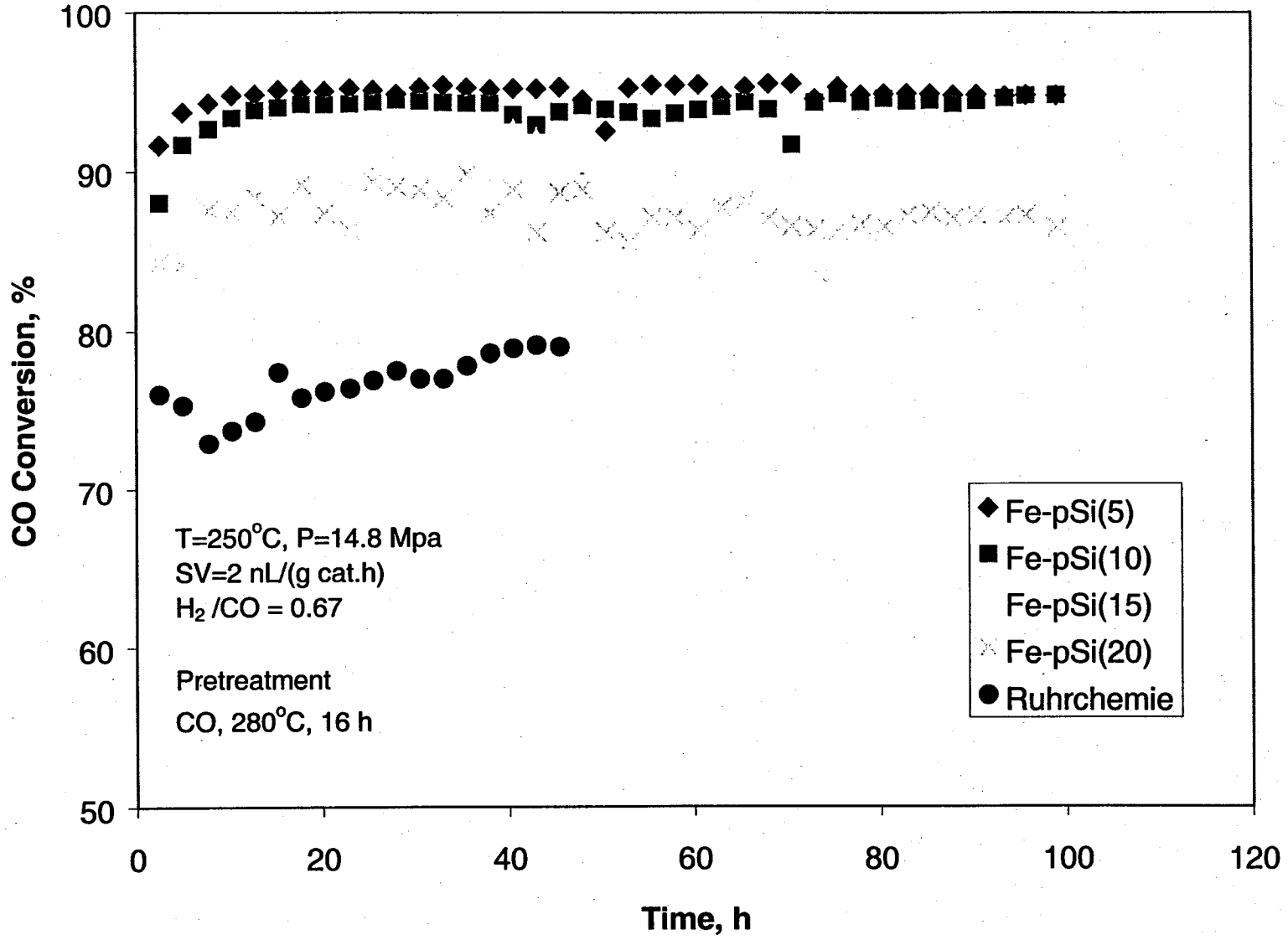


Figure 8. Effect of Precipitated Silica on Synthesis Gas Conversion and Catalyst Stability

Table 4. Catalyst Activity and Selectivity

| Catalyst Designation | CO Conversion (%)[a] | Selectivity | | | | α |
|---|---|---|---|---|---|---|
| | | $C_1$ | $C_2$-$C_4$ | $C_5$-$C_{11}$ | $C_{12}^+$ | |
| Fe-bSi(4) | 94.3 | 7.4 | 18.1 | 12.7 | 61.8 | 0.92 |
| Fe-bSi(8) | 94.1 | 6.8 | 17.6 | 13.0 | 62.5 | 0.91 |
| Fe-bSi(12) | 94.3 | 6.8 | 19.6 | 12.8 | 60.8 | 0.89 |
| Fe-bSi(16) | 95.5 | 9.9 | 25.0 | 17.3 | 47.8 | 0.87 |
| Fe-bSi(20) | 94.5 | 9.6 | 23.5 | 17.6 | 49.3 | 0.87 |
| Fe-pSi(5) | 95.5 | 8.8 | 23.2 | 22.0 | 46.0 | 0.87 |
| Fe-pSi(10) | 94.4 | 10.2 | 23.5 | 26.5 | 39.8 | 0.86 |
| Fe-pSi(15) | 90.1 | 10.2 | 22.4 | 30.5 | 36.9 | 0.87 |
| Fe-pSi(20) | 88.2 | 9.5 | 20.1 | 32.8 | 37.7 | 0.88 |
| HPR-43 | 95.0 | 3.9 | 17.7 | 23.8 | 54.6 | 0.90 |
| Ruhrchemie | 86 | 8.3 | 21.3 | 14.3 | 56.1 | 0.90 |

[a] Measured at 250°C, 1.48 MPa, 2 NL/g.cat/h, $H_2$/CO=0.67